Journal of Macromolecular Science, Part A

Publication details, including instructions for authors and subscription information:
http://www.informaworld.com/smpp/title~content=t713597274

Carrier-Mediated Transport of Hg(II) through Bulk and Supported Liquid Membranes

H. Korkmaz Alpoguz[a]; Ahmet Kaya[a]; Izzet Sener[a]
[a] Faculty of Sciences Arts, Department of Chemistry, Pamukkale University, Denizli, Turkey

To cite this Article Alpoguz, H. Korkmaz , Kaya, Ahmet and Sener, Izzet(2007) 'Carrier-Mediated Transport of Hg(II) through Bulk and Supported Liquid Membranes', Journal of Macromolecular Science, Part A, 44: 10, 1061 — 1068

To link to this Article: DOI: 10.1080/10601320701519559

URL: http://dx.doi.org/10.1080/10601320701519559

Journal of Macromolecular Science®, Part A: Pure and Applied Chemistry (2007) **44**, 1061–1068
Copyright © Taylor & Francis Group, LLC
ISSN: 1060-1325 print/1520-5738 online
DOI: 10.1080/10601320701519559

Carrier-Mediated Transport of Hg(II) through Bulk and Supported Liquid Membranes

H. KORKMAZ ALPOGUZ, AHMET KAYA, and IZZET SENER

Faculty of Sciences Arts, Department of Chemistry, Pamukkale University, Denizli, Turkey

Received March, 2007, Accepted April, 2007

The transport of Hg (II) ions from an aqueous solution into an aqueous receiving solution through bulk and supported liquid membranes containing a calix[4]arene derivative **1** as a carrier was examined. The kinetic parameters of bulk liquid membrane studies were analyzed assuming two consecutive, irreversible first-order reactions. The influence of temperature, stirring rate, carrier concentration and solvent on the kinetic parameters (k_1, k_2, R_m^{max}, t_{max}, J_d^{max}, J_a^{max}) has also been investigated. The membrane entrance rate, k_1, and the membrane exit rate, k_2, increased with increasing temperature and stirring rate. The activation energy values are calculated as 4.87 and 48.63 kj mol^{-1} for extraction and reextraction, respectively. The values of calculated activation energy indicate that the process is diffusionally controlled by species. Also, the transport behavior of Hg^{2+} from aqueous solution through a flat-sheet supported liquid membrane has been investigated by the use of calix[4]arene derivative **1** as carrier and Celgard 2500 as the solid support. A Danesi mass transfer model was used to calculate the permeability coefficients for each parameter studied. The highest values of permeability were obtained with 2-nitrophenyloctyl-ether (NPOE) solvent and the influence was found to be in the order of NPOE > chloroform > xylene.

Keywords: liquid membrane; calixarenes; transport of Hg (II); transport kinetics

1 Introduction

The toxicity of heavy metals is widely recognized due to their adverse effects upon human health. Mercury is a particularly toxic element of great environmental concern because it is widespread in the lithosphere and in water (1, 2). Inorganic mercury, especially soluble mercury species, can be transformed into methyl mercury by the action of microorganisms under aerobic conditions. The organomercury compounds thus formed have a strong tendency to accumulate as they pass through the food chain. Because of the great impact of mercury, there is an imperious need to determine and to recover it from water at low concentrations (2).

Calixarenes and derivatives can be used as receptors to recognize a wide variety of ions and guest molecules, forming host-guest or supramolecular complexes. This ability has been exploited in different fields and calixarenes and derivatives have been used extensively as selective ligands for a wide range of metal ions in liquid-liquid extraction, in selective transport, as ionophores in ion-selective electrodes and as chromophores in optical sensing (3, 4). Several studies have been published which make a case for calixarene derivatives as extractants for toxic metals (5–9).

Several technologies can be used to remove these toxic metals from liquid effluents, including precipitation, solvent extraction, ion exchange, etc., among these, the liquid membrane technique has acquired an importance for its use in separation, concentration or even analytical application. Though this technology is still in the research and development stage, it holds a deserving position in the field of membrane separations due to its advantages over conventional separation operations. Included in the liquid membrane characteristics are their high specificity, low energy utilization, ease of installation, etc. (10).

The different types of liquid membranes are reviewed in the literature (11, 12). Bulk liquid membranes usually consist of an aqueous donor and acceptor phase, separated by a water-immiscible liquid membrane phase in a U-tube. In supported liquid membranes, the extraction, stripping and regeneration of the organic phase are combined in a single stage (10).

Here, we report an investigation of co-transport of Hg^{2+} ion through liquid membranes. N,N′-bis(5-azo-25,26,27-tribenzoyloxy-28-hydroxycalix[4]arene)biphenyl **(1)** is the carrier ligand (as presented in Figure 1), which was synthesized according to the literature method (13). The kinetic

---

Address correspondence to: H. Korkmaz Alpoguz, Faculty of Sciences Arts, Department of Chemistry, Pamukkale University, 20017 Denizli, Turkey. E-mail: hkalpoguz@pau.edu.tr

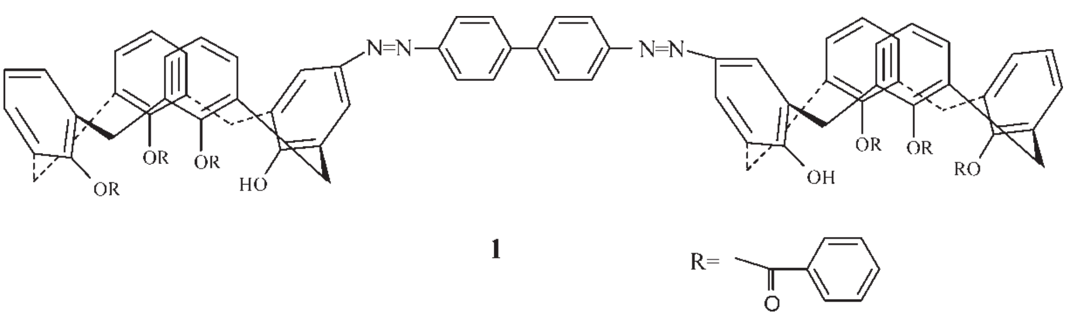

1

Fig. 1. The structure of calix[4]arene derivative **1** used as carrier.

parameters of bulk liquid membrane studies were analyzed assuming two consecutive, irreversible first-order reactions. Also, the transport behavior of Hg^{2+} from aqueous solution through a flat-sheet supported liquid membrane has been investigated by the use of calix[4]arene derivative **1** as carrier and Celgard 2500 as the solid support.

2 Experimental

2.1 *Materials*

The chemical reagents used in bulk liquid membrane experiments were mercury (II) nitrate (Merck), dichloromethane (Merck), chloroform (Merck), carbon tetrachloride (Merck) and picric acid, (Merck). Mercury (II) picrate solution was prepared by the addition of a 1×10^{-2} M mercury (II) nitrate to a 2.5×10^{-5} M aqueous picric acid solution and shaken at 25°C for 1 h. The aqueous solutions were prepared using demineralized water.

The chemical reagents used in supported liquid membrane experiments were mercury (II) nitrate, mecury (II) chloride and xylene were obtained from Merck Co., 2-nitrophenyl octyl ether from Fluka and used without further purification. The polymeric film Celgard 2500 (thickness: 25 μm, porosity 45%) was obtained from Celgard Inc. (Samples were kindly supplied by Oketek Co., Istanbul).

2.2 *Bulk Liquid Membrane Experiments*

Co-transport experiments were carried out in a U-type cell inserted inside a thermostated (Grand mark, model W14) apparatus (Figure 2). An organic solution (20 mL) containing the ionophore was placed in the bottom of the cell and two portions of aqueous donor and acceptor solutions (10 mL) were carefully added on top of them. Both surface areas were $2.5\ cm^2$. The organic phase was stirred at variable speeds magnetically (Chiltern mark, model HS 31).

The initial phases consisted of the donor phase, which was an aqueous mercury (II) picrate (2.5×10^{-5} M) solution, while the membrane phase was made up by dissolving carrier **1** in the organic phase. The acceptor phase consisted of doubly distilled water. Samples were taken from both water phases (acceptor and donor phases) at various intervals of time and the picrate ion concentration was analyzed by a spectrophotometric method. The spectrophotometric measurements were performed by means of an UV-Vis Spectrometer Shimadzu 160A. Experiments were performed with no carrier present, indicating that no transport of mercury (II) picrate occurred. The consecutive kinetic equations for a transport system were used by applying a simple theoretical approach which is discussed in detail elsewhere (14–20). The experiments were repeated at least three times.

The variation of the metal picrate concentration with time was directly measured in both the donor (C_d) and acceptor (C_a) phases. In the experiments, the variation of picrate ion concentration with time was directly measured in both donor (C_d) and acceptor phases (C_a). The corresponding change of picrate ion concentration in the membrane phase was determined from the material balance between the phases. For practical reason, the dimensionless reduced concentrations were used:

$$R_d = \frac{C_d}{C_{d0}} \quad R_m = \frac{C_m}{C_{d0}} \quad R_a = \frac{C_a}{C_{d0}} \qquad (1)$$

where C_{d0} is the initial Hg(II) ion concentration in the donor phase, while C_d, C_m and C_a represents the Hg^{2+} ion concentration in donor, membrane and acceptor phases, respectively. The material balance with respect to the reduced concentrations can be expressed as $R_d + R_m + R_a = 1$. From this expression, the kinetic behavior of

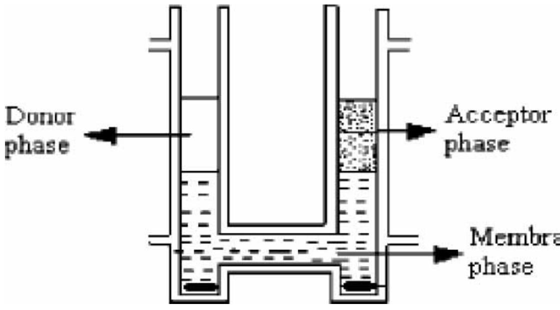

Fig. 2. Bulk liquid membrane apparatus for transport of Hg(II) ions; d, donor phase; a, acceptor phase; m, membrane phase.

the consecutive irreversible first order reactions can be described as follows;

$$C_d \xrightarrow{k_1} C_m \xrightarrow{k_2} C_a \quad (2)$$

where k_1 and k_2 are the apparent membrane entrance and exit rate constants, respectively. The kinetic scheme for consecutive reaction systems can be described by considering the reduced concentrations as follows;

$$\frac{d\,R_d}{dt} = -k_1 R_d \equiv J_d \quad (3)$$

$$\frac{d\,R_m}{dt} = k_1 R_d - k_2 R_m \quad (4)$$

$$\frac{d\,R_a}{dt} = k_2 R_m = J_a \quad (5)$$

where J represents the flux. When $k_1 \neq k_2$, integrating Equations (3–5), gives:

$$R_d = \exp(-k_1 t) \quad (6)$$

$$R_m = \frac{k_1}{k_2 - k_1}[\exp(-k_1 t) - \exp(-k_2 t)] \quad (7)$$

$$R_a = 1 - \frac{1}{k_2 - k_1}[k_2 \exp(-k_1 t) - k_1 \exp(-k_2 t)] \quad (8)$$

The kinetic parameters k_1 and k_2 were obtained by fitting Equations 6–8 to this data. As an example, the variation of the reduced concentration of Hg(II) ion through the liquid membrane with 1×10^{-4} M of carrier **1** in $CHCl_3$ at 300 rpm and 25°C is presented in Figure 3. The observed experimental results reveal that R_d decreases exponentially with time, accompanied by a simultaneous increase of R_a, whereas R_m presents at maximum at intermediate times.

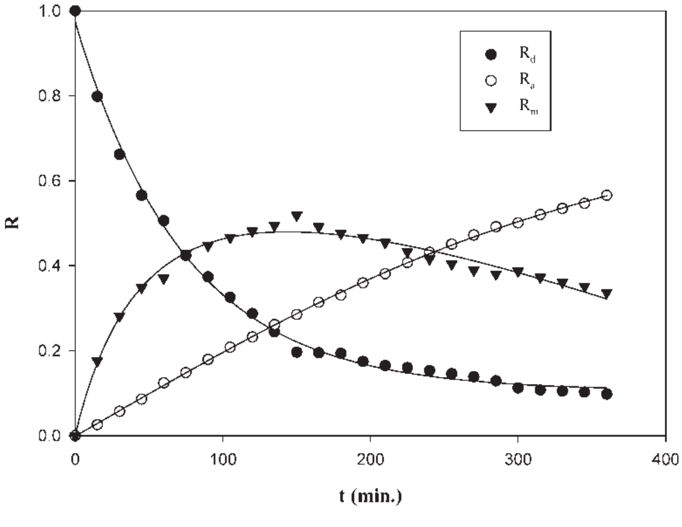

Fig. 3. Time dependence of R_d, R_m, and R_a for transport of Hg(II). Membrane: 1×10^{-4} M of carrier **1** in $CHCl_3$ (298 K and 300 rpm). Theoretical curves calculated from Equations (6–8).

The maximum values of R_m (when $dR_m/dt = 0$) and t_{max} may be written as follows:

$$R_m^{max} = \left(\frac{k_1}{k_2}\right)^{-k_2/(k_1-k_2)} \quad (9)$$

$$t_{max} = \left(\frac{1}{k_1 - k_2}\right) \ln\frac{k_1}{k_2} \quad (10)$$

By considering the first-order time differentiation of Equations. 6–8 at $t = t_{max}$, one obtains:

$$\left.\frac{d\,R_d}{dt}\right|_{max} = -k_1\left(\frac{k_1}{k_2}\right)^{-k_1/(k_1-k_2)} \equiv J_d^{max} \quad (11)$$

$$\left.\frac{dR_m}{dt}\right|_{max} = 0 \quad (12)$$

$$\left.\frac{dR_a}{dt}\right|_{max} = k_2\left(\frac{k_1}{k_2}\right)^{-k_2/(k_1-k_2)} \equiv J_a^{max} \quad (13)$$

We see that at $t = t_{max}$, the system is in steady state, because the concentration of Hg(II) ions in the membrane does not vary with time (Equation 12). Because the maximum entrance (J_d^{max}) and exit (J_a^{max}) fluxes are equal but having opposite signs:

$$-J_d^{max} = J_a^{max} \quad (14)$$

The actual numeric analysis was carried out by nonlinear curve fitting by using Sigma-Plot software program. The kinetic parameters k_1 and k_2 were obtained by fitting Equations (6–8) to this data. The activation energy values were obtained from the Arrhenius equation by using the k_1 and k_2 values at different temperature.

$$\ln(k) = \ln(A) - \frac{E_a}{RT} \quad (15)$$

2.3 Supported Liquid Membrane Experiments

The transport experiments were carried out in a permeation cell consisting of two identical cylindrical compartments (half-cell volume: 30 ml) (Figure 4), previously described (21). The supported liquid membranes consisted of a thin, microporous polypropylene film (Celgard 2500; thickness: 25 μm, porosity 45%) immobilizing the solution of carriers in organic solvents. Aqueous mercury (II) nitrate and mercury (II) chloride solutions were used as the feed phase, and deionized water was used as the stripping phase. The soaking time of the Celgard 2500 membrane is 24 h and the stirring speed is chosen as 300 rpm in the all transport experiments. The measurements were performed at a constant temperature of 25°C at least twice. The transported Hg^{2+} in nitrate and chloride salt forms was determined by monitoring the conductivity of the stripping phase as a function of time (Philips PW 9527 conductivity meter). The standard deviation in the transport measurements is about 15%.

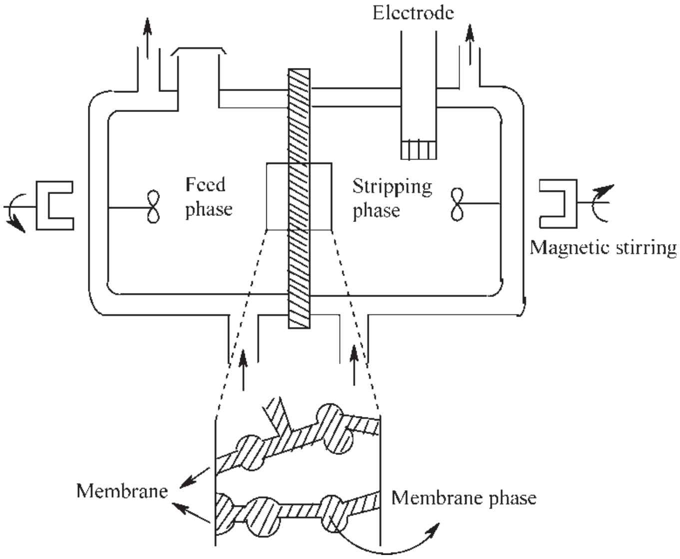

Fig. 4. Supported liquid membrane apparatus.

3 Results and Discussion

3.1 Bulk Liquid Membrane Studies

In our previous reports (14–16), the transport of Hg(II) ions from aqueous phase was carried out by using derivatives of calix[4]arenes as the carrier. In this work, the transport of Hg(II) ion by derivative of azo calix[4]arene in the liquid membrane was studied and the kinetic behavior of the transport process as a function of concentration, temperature, stirring rate, and solvents was investigated.

3.2 Effect of Carrier Concentration in Membrane on Transport of Hg(II) Ions

The carrier concentration of organic phase has a significant effect on the metal ion transport across the membrane. It is generally expected to increase with the carrier concentration. The transport experiments were carried out at three different initial carrier **1** concentrations 1×10^{-6}, 1×10^{-5}, and 1×10^{-4} M in $CHCl_3$ at 298 K and 300 rpm. The obtained kinetic parameters for the effect of concentration of carrier **1** are presented in Table 1. It was found that the initial carrier concentration influences the kinetic constants, as well as flux values, in full agreement with previously obtained results (9, 14–16). It can be seen that, both kinetic constants k_1 and k_2 or fluxes are dependent on the carrier concentration and increases steadily with the initial carrier concentration, as shown in Figure 5. It had been reported that in controlled conditions, k_1 and k_2 increases with increasing carrier concentration, showing small and fractional exponent value (22). This obviously can be assumed from Equations (6–8) that the reduced dimensionless concentration is related with the carrier concentration.

In addition, a blank experiment was performed with no carrier present in the membrane. No detectable movement of the Hg(II) ions through the liquid membrane was found in the blank experiment, suggesting that the transport of Hg(II) ions through the liquid membrane is fulfilled by the carrier.

3.3 Effect of Temperature on Transport of Hg(II) Ions

The effect of temperature on the transport of Hg(II) ions across the bulk liquid membrane was tested at 293, 298, 303 and 308 K, respectively. The experimental results are shown in Table 2. It is quite obvious that k_1 and k_2 increases with an increase in the temperature. Table 2 also shows that t_{max} and R_m^{max} decreases with an increase of temperature. The maximum R_m values were found to lie between the 0.39 and 0.55 ranges. This shows that the membrane phase was also effect on the transport. It is also seen that the t_{max} values was decreased upon increasing of temperature. It is immediately obvious that the extraction of Hg^{2+} from the donor phase into the membrane occurs at a rate equal to the release of mercury from the membrane into the acceptor phase. As known, activation energy values are quite low for diffusion-controlled processes, whose rate constants are strongly affected by temperature. The E_a values of diffusion-controlled processes are lower than those of chemically controlled processes. It was pointed out that the activation energies of diffusion-controlled processes are lower than 20 kcal mol^{-1} (23). The activation energy values were obtained from the Arrhenius equation by using the k_1 and k_2 values at different temperature. An Arrhenius-type plot is followed perfectly in Figure 6. The activation energy values are 4.87 and 48.63 kj mol^{-1} for extraction and reextraction, respectively. The calculated activation energy shows that the transport of Hg^{2+} ions is diffusion controlled processes (23).

3.4 Effect of Stirring Rate on Transport of Hg(II) Ions

The influence of the stirring speed on Hg(II) ions transport was studied in order to optimize uniform mixing of the

Table 1. The kinetic parameters for Hg(II) ions at different carrier **1** concentrations in $CHCl_3$ (298 K and 300 rpm)

Concentration (M)	$k_1 \times 10^3$ (min^{-1})	$k_2 \times 10^3$ (min^{-1})	R_m^{max}	t_{max} (min)	$J_d^{max} \times 10^3$ (min^{-1})	$J_a^{max} \times 10^3$ (min^{-1})
1×10^{-6}	1.12	3.64	0.18	467.14	−0.66	0.66
1×10^{-5}	3.55	4.16	0.34	260.00	−1.41	1.41
1×10^{-4}	9.69	4.38	0.52	149.53	−2.28	2.28

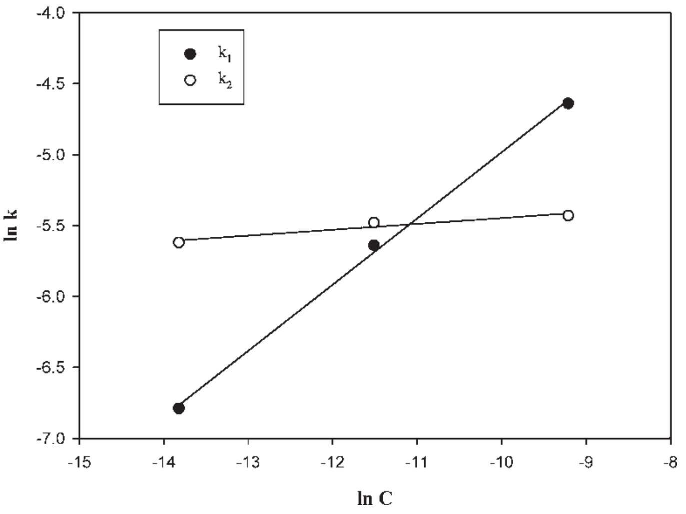

Fig. 5. Concentration dependence of k_1 and k_2 for transport of Hg(II) (298 K and 300 rpm in $CHCl_3$).

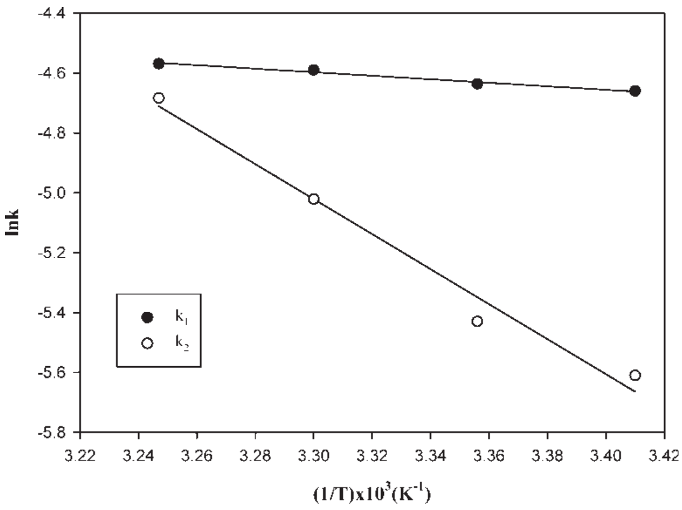

Fig. 6. Arrhenius plots for transport of Hg(II) in liquid membrane. Membrane: 1×10^{-4} M of carrier **1** in $CHCl_3$ at 300 rpm.

solution and to minimize thickness of aqueous boundary layers. In the present investigation, the stirring rate of the membrane phase was carried out at three different stirring rate, 200, 300, and 400 rpm at 298 K when the carrier **1** concentration was 1×10^{-4} M in $CHCl_3$. The results are presented in Table 3, indicate that the stirring rate affects the transport rate of Hg(II) through the liquid membrane. As shown in Table 3, the membrane entrance (k_1) and exit (k_2) rate constants increased by rising stirring rate.

3.5 Effect of Solvent on Transport of Hg(II) Ions

The experiments were accomplished with three different solvents: CH_2Cl_2, $CHCl_3$ and CCl_4. The kinetic parameters are shown in Table 4 and Figure 7, indicate that the highest efficiency has been obtained with CH_2Cl_2. It is also found that the membrane entrance and exit rate constants, as well as the flux values vary in order of $CH_2Cl_2 > CHCl_3 > CCl_4$. In the ion transport, the polarity and viscosity of solvents are very important. Due to the highest polarity and the lowest viscosity of CH_2Cl_2, it is the most effective solvent. This result is in harmony with the previous studies (9, 14–16).

3.6 Supported Liquid Membrane Studies

The transport experiments were carried out with an apparatus designed by Reinhoudt et al. (21) shown as in Figure 3. The organic phase impregnated a microporous support of polypropylene placed between the aqueous phases. The mass of organic phase incorporated in a membrane was determined by weighing the membrane before and after impregnation.

We have induced a coupled co-transport of Hg^{2+} ion and nitrate and chloride anions, establishing a chemical gradient between the feed and stripping solutions. According to the mass transfer model described by Danesi (24), the permeability (P) is obtained using Equations (16) and (17).

$$\text{Feed Solution}: \ln\left(\frac{C}{C_0}\right) = -\varepsilon\frac{S}{V_B}P_F t \qquad (16)$$

$$\text{Strip Solution}: \ln\left(1 - \frac{C'}{C_0}\right) = -\varepsilon\frac{S}{V_A}P_S t \qquad (17)$$

The initial flux of Hg^{2+} J_i is obtained by Equation (18):

$$Ji = PC*/1 \qquad (18)$$

Where C/C′: concentration of the cation, respectively in the feed/stripping solution at time t; C_0: initial concentration

Table 2. The kinetic parameters of Hg(II) transport using carrier **1** at different temperatures (Stirring rate is 300 rpm; solvent is $CHCl_3$).

Temperature (K)	$k_1 \times 10^3$ (min^{-1})	$k_2 \times 10^3$ (min^{-1})	R_m^{max}	t_{max} (min)	$J_d^{max} \times 10^3$ (min^{-1})	$J_a^{max} \times 10^3$ (min^{-1})
293	9.47	3.66	0.55	163.67	−2.01	2.01
298	9.69	4.38	0.52	149.53	−2.28	2.28
303	10.15	6.60	0.45	121.25	−2.96	2.96
308	10.37	9.24	0.39	102.09	−3.60	3.60

Table 3. The kinetic parameters of Hg(II) transport using carrier **1** at different stirring rates (T = 298 K; solvent is $CHCl_3$)

Stirring rate (rpm)	$k_1 \times 10^3$ (min^{-1})	$k_2 \times 10^3$ (min^{-1})	R_m^{max}	t_{max} (min)	$J_d^{max} \times 10^3$ (min^{-1})	$J_a^{max} \times 10^3$ (min^{-1})
200	8.56	3.62	0.53	174.21	−1.93	1.93
300	9.69	4.38	0.52	149.53	−2.28	2.28
400	11.5	12.79	0.35	82.42	−4.45	4.45

Table 4. The kinetic parameters for Hg(II) transport using carrier **1** when different solvents are used (298 K and 300 rpm)

Solvent	$k_1 \times 10^3$ (min^{-1})	$k_2 \times 10^3$ (min^{-1})	R_m^{max}	t_{max} (min)	$J_d^{max} \times 10^3$ (min^{-1})	$J_a^{max} \times 10^3$ (min^{-1})
CH_2Cl_2	19.72	16.68	0.40	55.07	−6.66	6.66
$CHCl_3$	9.69	4.38	0.52	149.53	−2.28	2.28
CCl_4	0.64	0.95	0.30	1274.81	−0.28	0.28

of the cation in the feed solution; ε: porosity of supported liquid membrane (%); S: membrane surface area (cm^2); V: volume of feed or stripping solution (cm^3); C*: the concentration of carrier in the membrane.

P_F and P_S were determined graphically from the slope of plots $\ln(C/C_0)$ and $\ln(1 - C'/C_0)$, respectively vs. t. In ideal cases, P_F is equal to P_S.

In this study, supported liquid membrane transport works for Hg(II) have been carried out by using Celgard 2500 model membrane and permeabilities and fluxes have been determined by using versatile metal salts ($Hg(NO_3)_2$, $HgCl_2$) and different solvents (xylene, chloroform and 2-nitrophenyl octyl ether).

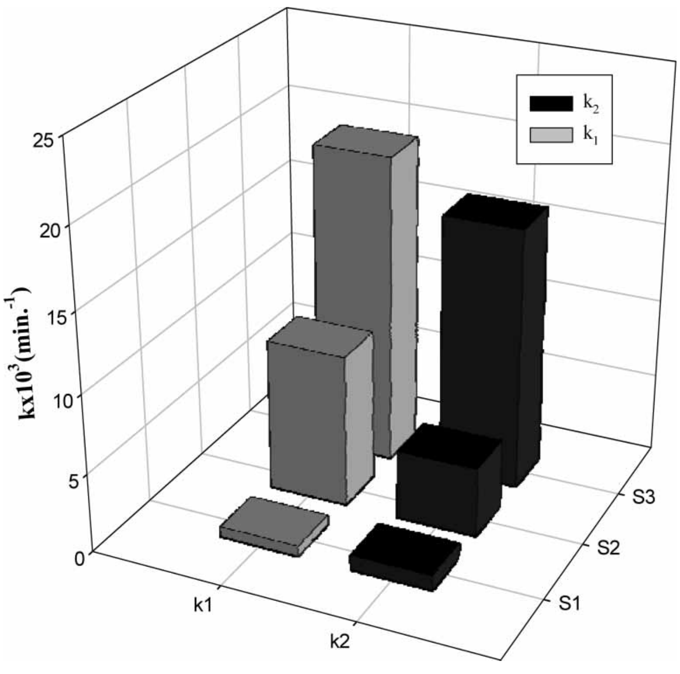

Fig. 7. Solvent dependence of k_1 and k_2 for transport of Hg(II) ions, where S1, S2 and S3 are CCl_4, $CHCl_3$ and CH_2Cl_2, respectively. Conditions of experiments, see Table 4.

Depending upon these results, plots of $\ln(1 - C'/C_0)$ vs. time for the nitrate and chloride salts of the Hg^{2+}, together with the carrier **1** in NPOE solvent using Celgard 2500 as solid support membrane are presented in Figures 8 and 9. Both plots give a straight line with slopes, which verify that the transport efficiency depends upon the type of anion and solvent. The values of permeabilities (P) and fluxes (J_i) are given in Table 5.

The liquid membrane technique contains two processes in a single stage: extraction of metal ion from the aqueous feed solution to the organic phase containing the carrier molecules (membrane) and a reextraction of this metal ion from the membrane to the aqueous stripping phase. The overall transport process consists of a mixture diffusion steps and complexations/decomplexation reactions at two independent and possible different interfaces.

The mechanism of the ion pair mediated transport (co-transport) is given in Figure 10. L represents the ligand carrier. At the interface between feed and membrane,

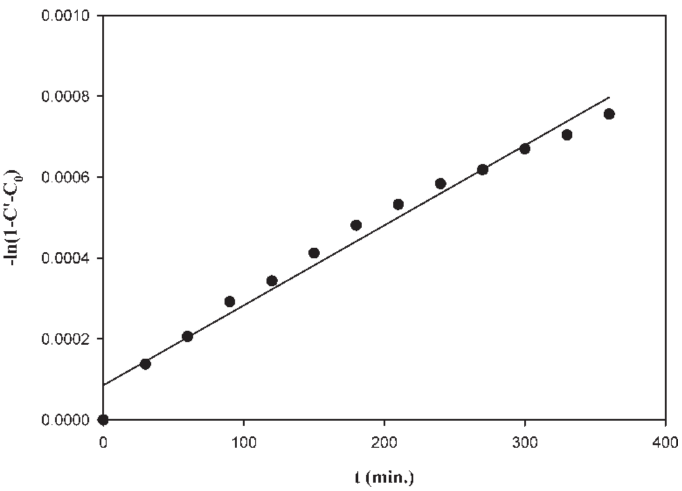

Fig. 8. Hg^{2+} transport experiment with calix[4]arene derivative **1** for Celgard 2500 membrane. Feed solution: 0.01 M $Hg(NO_3)_2$, organic membrane: $\mathbf{1} = 10^{-3}$ M in NPOE, stripping solution: Deionize water, $V_F = V_S = 30$ cm^3, S = 9.08 cm^2, $\varepsilon = 0.45$.

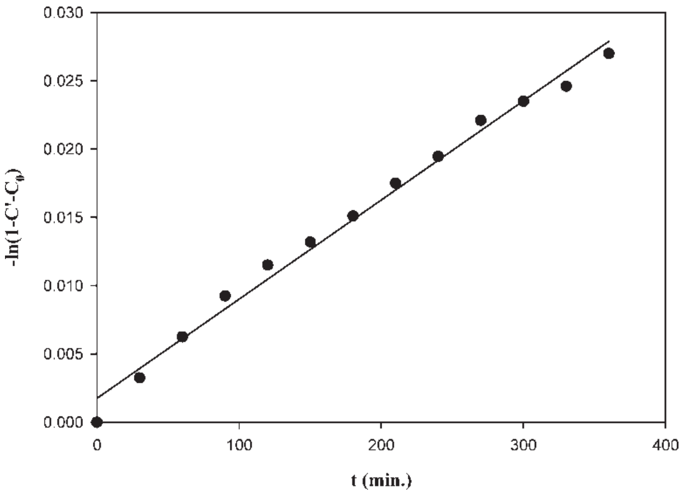

Fig. 9. Hg^{2+} transport experiment with calix[4]arene derivative **1** for Celgard 2500 membrane. Feed solution: 0.01 M $HgCl_2$, organic membrane: **1** $=10^{-3}$ M in NPOE, stripping solution: Deionize water, $V_F = V_S = 30\ cm^3$, $S = 9.08\ cm^2$, $\varepsilon = 0.45$.

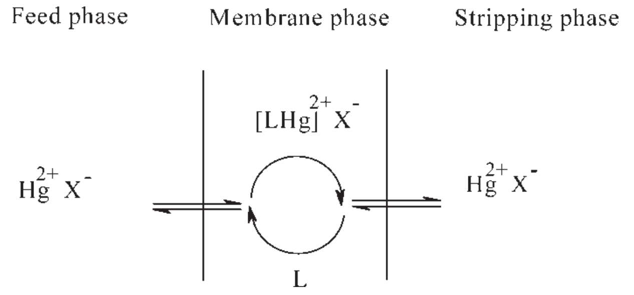

Fig. 10. Mechanism of the ion pair mediated transport (co-transport) of Hg^{2+} through supported liquid membrane X^-: Cl^-, NO_3^-, L: Ligand, $[L\text{-}Hg]^{2+}X^-$: ion pair.

$Hg^{2+}X^-$ ion pair forms (X:Cl^- or NO_3^-) complex with ligand, then the $[LHg]^{2+}X^-$ complex diffuses through the membrane. At the interface between membrane and stripping, the carrier ion pairs are decomplexed and $Hg^{2+}X^-$ is liberated into the stripping phase. Finally, the ligand carrier diffuses back across the membrane aqueous boundary layers.

When compared with the chloride and nitrate forms, the transport of Hg^{2+} was found to be higher in the chloride form. These results can be ascribed to the low solubility of $(NO_3)^-$ in organic phase by the polarity of co-transport ion and it could also be explained by the fact that the radius of chloride anion (0.168 nm) is smaller more than that of nitrate anion (0.200 nm).

When the different solvents were used for carrier **1**, the values of permeabilities and fluxes obtained were also different. It has been previously pointed out that the nature of solvent has a great influence on the transport efficiency through bulk liquid membranes (9, 14–16, 20). The results obtained for permeability and flux with solvents are presented in Table 5. It is apparent from the results that the permeability and fluxes values are remarkably different in different solvents and found to be in the order of NPOE > chloroform > xylene. In the case of xylene and chloroform, the values of permeabilities and fluxes are smaller than that of NPOE. Nitrophenyl alkyl ethers (NPHE-hexyl; NPOE-octyl) were used for supported liquid membrane studies because they lead to a stable membrane due to their very low solubility in water (25–28). Also, the polymeric support materials used are very important in the stability of the membrane. The requirement for a good polymeric support are high porosity, small pore size, good mechanical strength, chemical resistance, thinness, hydrophobicity, and low cost.

Table 5. Permeabilities (P) and fluxes (J_i) for transport through supported liquid membranes by calixarene derivative **1** for Celgard 2500 membrane.

Ligand	Ion pair	Solvent	$P \times 10^5$ $(cm \cdot dk^{-1})$	$J_i \times 10^5$ $(mol \cdot L^- \cdot dk^-)$
1	$Hg(NO_3)_2$	Xylene	0.24	0.94
		Chloroform	0.34	1.37
		NPOE	1.45	5.81
1	$HgCl_2$	Xylene	6.59	26.36
		Chloroform	11.05	44.12
		NPOE	53.18	213.27

4 Conclusions

The Hg(II) ions can be effectively transported through a bulk and supported liquid membranes containing calix[4]arene derivative **1**. The efficiency of the methods depends on various parameters, i.e., the carrier concentration, type of solvent and anion, stirring speed, temperature.

5 References

1. Mason, R.P., Reinfelder, J.R. and Morel, F.M.M. (1995) *Water Air Soil Pollut.*, **80**, 915.
2. Shamsipur, M., Hashemi, O.R. and Lippolis, V. (2006) *J. Membr. Sci.*, **282**, 322.
3. Reinhoudt, D. (1995) *Sens. Actuators B*, **24–25**, 197.
4. Mathew, V.J. and Khopkar, S.M. (1997) *Talanta*, **44**, 1699.
5. Schazmann, B., O'Malley, S., Nolan, K. and Diamond, D. (2006) *Supramolecular Chem.*, **18**, 515.
6. Memon, S. and Yilmaz, M. (2000) *Sep. Sci. Technol.*, **35**(**3**), 457.
7. Memon, S., Uysal, G. and Yilmaz, M. (2000) *Sep. Sci. Technol*, **35**(**8**), 1247.
8. Uysal, G., Memon, S. and Yilmaz, M. (2001) *React. Funct. Poly.*, **47**(**3**), 165.
9. Alpoguz, H.K., Kaya, A., Yilmaz, A. and Yilmaz, M. (2005) *J. Macromol. Sci. Part A: Pure Appl. Chem.*, **A42**, 577.
10. Alonso, M., Delgado, A.L., Sastre, A.M. and Alguacil, F.J. (2006) *Chem. Engineering J.*, **118**, 213.
11. Sastre, A.M., Kumar, A., Shukla, J.P. and Sing, R.K. (1998) *Sep. Purif. Meth.*, **27**, 213.

12. Ho, W.S.W. (2003) *Ann. NY Acad. Sci.*, **984**, 97.
13. Tilki, T., Şener, İ, Karcı, F., Gülce, A. and Deligöz, H. (2005) *Tetrahedron*, **61**(**40**), 9624.
14. Alpoguz, H.K., Memon, S., Ersoz, M. and Yilmaz, M. (2002) *New J. Chem.*, **26**(**4**), 477.
15. Alpoguz, H.K., Memon, S., Ersoz, M. and Yilmaz, M. (2004) *Sep. Sci. Technol.*, **39**(**4**), 799.
16. Alpoguz, H.K., Kaya, A. and Deligöz, H. (2006) *Sep. Sci. Technol.*, **41**, 1155.
17. Szpakowska, M. and Nagy, O.B. (1999) *J. Phys. Chem. A*, **103**, 1553.
18. Szpakowska, M. and Naggy, O.B. (1990) Copper(II) ion transport mono and binary liquid membranes. *Bull. Soc. Chim. Belg.*, **99**(**4**), 243.
19. Szpakowska, M. (1994) *J. Membr. Sci.*, **92**(**3**), 267–273.
20. Alpaydin, S., Yilmaz, M. and Ersoz, M. (2004) *Sep. Sci. Technol.*, **39**(**9**), 2189.
21. Visser, H.C., Reinhoudt, D.N. and Dejong, F. (1994) *Chem. Soc. Rev.*, **23**, 75–81.
22. Szpakowska, M. and Nagy, O.B. (2000) *J. Membr. Sci.*, **168**(**1–2**), 183.
23. Lazarova, Z. and Boyadzhiev, L. (1993) *J. Membr. Sci.*, **78**(**3**), 239.
24. Danesi, P.R. (1984) *Sep. Sci. Technol.*, **19**, 857.
25. Arnaud-Neu, F., Böhmer, V., Dozol, J.F., Grüttner, C., Kraft, R.A., Mauprivez, D.O., Rouquette, H., Schwing-Weill, M.J., Simon, N. and Vogt, W. (1996) *J. Chem. Soc. Perkin Trans. 2*, **2**(**6**), 1175.
26. Casnati, A., Pochini, A., Ungaro, R., Ugozzoli, F., Arnaud-Neu, F., Fanni, S., Schwing, M.J., Egbering, R.J.M., Jong, F. and Reinhoudt, D.N. (1995) *J. Am. Chem. Soc.*, **117**, 2767.
27. Dozol, J.F., Simon, N., Lamare, V., Rouquette, H., Eymard, S., Tournois, B., Marc DCC/DESD/SEP, D.D. and Macias, R.M. (1999) DIST/UDC. *Sep. Sci. Technol.*, **34**(**6**&**7**), 877.
28. Kim, J.K., Kim, J.S., Shul, Y.G., Lee, K.W. and Oh, W.Z. (2001) *J. Membr. Sci.*, **187**, 3.